Analysis of Wetting Transition and Pattern Collapse During the Drying Process of Deep Trench Isolation Structures Using Ultra-high Frequency Acoustic Waves and SEM Imaging

Abbas Salhab, Julien Carlier, Malika Toubal, Pierre Campistron, Marc Neyens, Bertrand Nongaillard, Vincent Thomy

16ème Congrès Français d'Acoustique
11-15 Avril 2022, Marseille

Analysis of Wetting Transition and Pattern Collapse During the Drying Process of Deep Trench Isolation Structures Using Ultra-high Frequency Acoustic Waves and SEM Imaging.

A. Salhab[*a], J. Carlier[a], M. Toubal[a], P. Campistron[a], M. Neyens[b], B. Nongaillard[a], V. Thomy[a]

[a] Univ. Polytechnique Hauts-de-France, Univ. Lille, CNRS, Centrale Lille, UMR 8520 - IEMN-Institut d'Electronique de Microélectronique et de Nanotechnologie, F-59000
[b] STMicroelectronics, 850 rue Monnet, F-38926 Crolles, France

Removing contaminants from silicon wafers surface is an important part in the semi-conductors industry. Thus through wet cleaning processes, after each operation (lithography, etching, etc…), contaminants like metals, organic impurities and dopants need to be removed. A drying process is also necessary after each of these wet operations in order to remove the cleaning chemicals used. These two processes (wet cleaning and drying) are critical when dealing with micro / nanoscale geometries that have high aspect ratio, making removal of small particles a tedious task that can create several problems (inefficient cleaning and surface modification). Wetting characterization using liquid flow on surface of Deep Trench Isolation (DTI) structures used in STMicroelectronics image sensors has already been studied. The dynamic study was carried out using ultra-high frequency (#GHz) acoustic waves and micro-fluidic channel made of PolyDimethylSiloxane (PDMS), in which we observed some surface modification of the DTI during the drying process. In this paper we examine in depth the drying phenomenon of the DTI, and we show the wetting state transition of the DTI from partial wetting to quasi-complete and sometimes complete wetting state. Also, we analyze the effect of capillary forces on micro / nano-structures deformation known as pattern collapse. This study is based on the correlation of a set of acoustic measurements with electron microscopy (SEM) images.

1 Introduction

The trend in the semiconductor industry is to make smaller structures as the size of electronic components such as transistors continues to decrease reaching sizes of some nanometers. This trend in size reduction lead to higher aspect ratio (AR) which is defined as the ratio of height to lateral dimension of the structure. Thus when making patterned (etched) silicon (Si) wafers, it is therefore crucial to establish efficient cleaning (complete wetting) and drying processes of these silicon structures. However, these high AR make it difficult to penetrate the liquid inside the structures as well as making them susceptible to deformation due to high capillary forces of the liquid during the drying process. On one hand, to remove organic impurities and metal contamination, the complete liquid penetration into the silicon structures is desired. On the other hand, after the wet cleaning process is done, efficient and uniform drying of these high AR structures is desired to prevent structural deformation known as pattern collapse.

To understand and optimize these phenomena it is essential to characterize the wettability of solid surfaces. In the case of a smooth surfaces, the wettability can be judged based on the Young's contact angle *"θ"* [1], where a surface is said to be either hydrophilic "wettable" ($\theta < 90°$) or hydrophobic "non-wettable" ($\theta > 90°$). In case of textured surfaces, the wetting characterization is more challenging in a sense that we could have multiple wetting states. For example, studying wetting transition from Cassie-Baxter [2] to Wenzel state [3] is important to see what factors control this transition and to prevent it when designing superhydrophobic textured surface for applications such as waterproof textiles [4] and drag reduction [5]. Other applications, such as cleaning processes need to promote Wenzel state for liquid total impregnation inside the structuration.

The characterization of such wetting states is still challenging and numerous methods have been developed based on different physical effect. ATR-FTIR (Attenuated Total Reflectance-FTIR) [6] and EIS (Electrochemical Impedance Spectroscopy) [7] are some of the methods that could give real-time wetting characterization of micro / nanometric structured interfaces.

In our study, we will monitor the wetting transition on the Deep Trench Isolation (DTI) structures with different AR by ultra-high frequency acoustic reflectometry method. The DTI is used as pixel insulator in image sensors and the efficient cleaning of such structures is important to prevent the apparition of white pixels on images. In addition, we will use a PolyDiMethylSiloxane (PDMS) based micro-channel system to inject the liquid on the surface of the DTI in order to study the wetting process using flow conditions as close as possible to those used at STMicroelectronics. Finally, the use of Scanning Electron Microscopy (SEM) images on the DTI will enable us to detect pattern collapse.

2 Experimental setup

2.1 DTI geometry

The DTI structures are etched inside matrices found on the frontside of 300 mm diameter silicon (Si) wafer of 785 ± 5 µm thickness made by STMicroelectronics. They are composed of 200 nm wide and 4 µm to 7 µm deep trenches (Figure 1). On the top surface of the trenches, three layers composed of 7.5 nm silicon dioxide (SiO_2), 55 nm silicon nitride (Si_3N_4) and 80 ± 20 nm (SiO_2) are stacked respectively (Figure 2).

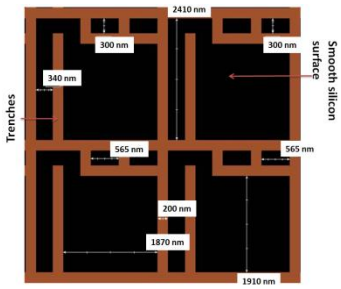

Figure 1 – SEM image of the DTI geometry found inside the etched matrices.

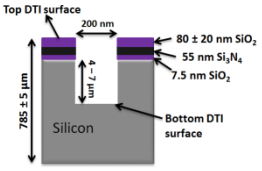

Figure 2 – Schematic of the trench structure

2.2 PDMS micro-channel

We create a fluidic channel whose dimensions and flow parameters allow finding the cleaning conditions applied in industry. Thus an 80 µm deep PDMS micro-channel mold is fabricated by laser lithography starting from SU-8 2075 resist (Kayaku advanced materials Inc.). The micro-channel mold 3.1 x 3.3 mm^2 lateral dimensions are chosen so that it can cover the all the surface area of the 2.1 x 2.3 mm^2 DTI matrix (Figure 3).

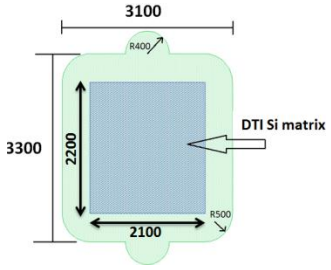

Figure 3 – Schematic of the micro-channel covering the DTI matrix. Dimensions are given in micrometers.

In the industrial single wafer cleaning process, the liquid film thickness "*h*" can change depending on the distance from the wafer's center "*r*", flow rate "*Q*", liquid kinematic viscosity "*ν*" and the rotational speed of the wafer "*ω*" (Figure 4.a). The micro-channel thickness is taken as "2*h*" to have the same velocity profile distribution as the single wafer system (Figure 4.b). The liquid film thickness "*h*" is related to the different parameters by [8]:

$$h = 0.782 \times Q^{0.33} \times \nu^{0.33} \times \omega^{-0.67} \times r^{-0.67} \qquad (1)$$

The 80 µm (2*h*) depth of the micro-channel is calculated for the following parameters values: Q = 0.12 $L.min^{-1}$, ν = 1.10^{-6} $m^2.s^{-1}$ (water at 20 °C), ω = 800 r.p.m. and r = 50 mm.

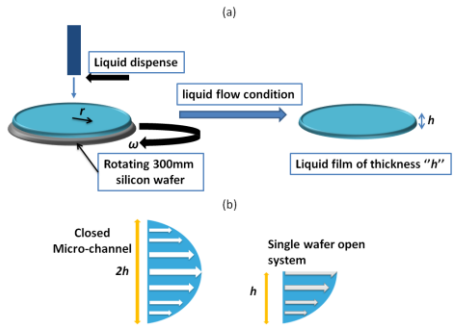

Figure 4 – (a) Schematic of the liquid film formed during the rotation of wafer in the industrial single wafer cleaning process (b) schematic of velocity distribution in the micro-channel and the single wafer system.

After preparing the mold, the next step is the preparation of the PDMS mixture. First 30 g of the PDMS base is added into a cup then 1/10 of the amount PDMS curing agent is added into the same cup (3 g). Then the cup is putted into a planetary mixer (ARV310, Thinky USA, INC) for about 1 minute under a vacuum pressure of 30 KPa and a rotational speed of 2000 r.p.m. The purpose of this operation is that, both liquids (base and curing agent) will be properly mixed and that the air bubbles in the resulting solution will be also removed under vacuum.

The PDMS solution is then poured on the mold and put in an oven at 70 °C for 3 hours to polymerize the PDMS. After the heating process, the PDMS which contain the micro-channel pattern is detached from the mold. Then using a biopsy punch with diameter equal to 2 mm, the inlet and outlet of the micro-channel is drilled into the PDMS.

Then, the surface of the PDMS micro-channel is treated with Electro-Technic Products (Chicago, IL) hand-held corona plasma discharge for 1 minute. Then the PDMS micro-channel is immediately placed over the DTI silicon wafer at the specified position in order to cover the DTI matrix. Upon contact, a bridging bond Si-O-Si is created at the interface making an irreversible seal. Note that the surface of the DTI wafer was not exposed to the plasma O_2 since it can transform the surface to hydrophilic changing its wettability. The last step includes heating the DTI wafer in an oven at 70 °C for 1 hour to strengthen the bond with PDMS micro-channel.

2.3 Acoustic reflectometry method

The acoustic reflectometry method for wetting characterization developed at the IEMN laboratory [9], consists of using ultra-high frequency longitudinal incident waves generated by piezoelectric transducers built on the backside of a 7 x 7 cm^2 patterned silicon wafer.

The piezoelectric transducers are made up of three layers. First, a ground electrode deposited on silicon by thermal evaporation (10 nm titanium "Ti" + 50 nm platinum "Pt"). The transducers are circular in shape (100 µm in diameter) and defined in shape and size by a photolithography process. Another layer of zinc oxide (ZnO) is deposited on top of the ground electrode by magnetron sputtering.

The thickness of the ZnO will determine the central frequency of the transducer. In this work we deposited a thin film (thickness of about 330 nm) of ZnO which will give us transducers generating longitudinal waves of 4 GHz for the central frequency. This central frequency corresponds to a wavelength of 2.1 µm in the silicon, smaller than the etch depth (4 µm) to ensure the separation of echoes between the top and bottom surface of the DTI (Figure 2). A final layer of top electrode is deposited by thermal evaporation (50 nm Pt). The different thicknesses of the materials have been predicted by a simulation to achieve the maximum conversion of electrical energy into acoustic energy [10]. The incident longitudinal waves will be reflected at the bottom and top surface of the trenches generating two different echoes A_{11} and A_{12} respectively (Figure 5). Depending on the medium present at the interface (air or liquid), the surface characterization is done by measuring the electrical impedance of the transducer. The measurement procedure is done by first measuring the scattering parameter $S_{11}(f)$ (ratio of complex voltage of reflected to incident waves) using a SussMicrotech probe coupled with a Rhode & Schwarz 300 kHz – 8 GHz Vector Network Analyzer (VNA). Using an inverse Fourier

transform to $S_{11}(f)$, the reflected echoes (A_{11} and A_{12}) are obtained in the time domain $S_{11}(t)$. To obtain the acoustic reflection coefficients, the amplitude of the signal is then normalized to air in order to eliminate any intrinsic insertion losses related to the measurements. The reflection coefficients on the bottom and top surface of the DTI (r_1 and r_2 respectively) are given as:

$$|r_1| = \frac{A_{11}^{liquid}}{A_{11}^{air}} \quad and \quad |r_2| = \frac{A_{12}^{liquid}}{A_{12}^{air}} \qquad (2)$$

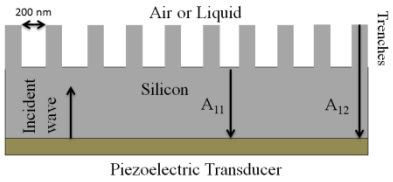

Figure 5 – Schematic of acoustic reflectometry method in wetting characterization of textured interfaces.

The final system (PDMS micro-channel + piezoelectric transducer + (7 x 7) cm^2 DTI wafer) is shown in Figure 6. To control the liquid flow inside the micro-channel, a microfluidic system MFCS-FLEX (from Fluigent company) is used by varying the pressure from some mbar up to 1 bar. The liquid will fill the micro-channel at a pressure of 300 mbar through a series of microfluidic tubes (0.5 mm internal diameter with 0.8 mm wall thickness) then air will be sent at a pressure of 1 bar to dry the liquid from the micro-channel.

The VNA is connected to a MatLab program which get the $S_{11}(t)$ data and enable the direct calculation of r_1 and

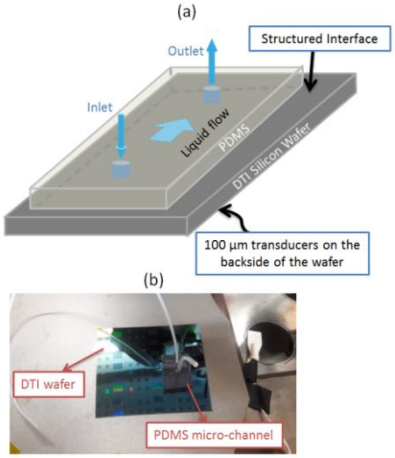

Figure 6 – (a) Schematic of the DTI wafer coupled with PDMS micro-channel and transducers (b) image of a DTI wafer sample with micro-channel attached to it.

r_2 with an acquisition time of 12 s.

The measurement procedure is done in three phases:

- Phase 1 : r_1 and r_2 are measured with time before injecting liquid in the micro-channel (air present: $r_1 = r_2 = 1$),
- Phase 2 : liquid is injected in the micro-channel and the changes of the reflections coefficients are measured with time,
- Phase 3: air is injected to dry the micro-channel where r_1 and r_2 are measured until returning to phase 1 ($r_1 = r_2 = 1$).

The automated acquisition with MatLab will enable us to monitor the wetting transition inside the DTI with a time delay of 12 s.

The measurements are done at 20 °C on four DTI samples with different etch depth (4, 5, 6 and 7 µm) and using different ethanol (EtOH) / distilled water (DW) mixtures (surface tension decreases as the ethanol concentration increases). A diluted version of the Standard Clean 1 (SC1) solution used at STMicroelectronics to eliminate organic and oxide contaminations, is also used for the measurements. The SC1 will be composed of: 80 parts H_2O, 1 part ammonia solution (NH_4OH (30%)) and 2 parts hydrogen peroxide solution (H_2O_2 (30%)).

A highly diluted version of the SC1 is used in order to avoid basic pH as it can damage the PDMS micro-channel.

3 Results and discussion

3.1 Wetting transition

The measurements were carried out with 100 µm diameter transducers, with about a 4 GHz central frequency within the band [1 GHz; 6 GHz].

First, experimental measurements using different EtOH / DW mixtures on four different trenches depths DTI wafers (4 µm, 5 µm, 6 µm and 7 µm) were carried out. Each solution was injected into the micro-channel at a pressure of 300 mbar and air is injected at 1 bar between each solution to dry up the micro-channel.

The measurements of the acoustic reflection coefficient r_1 using water/ethanol mixtures are shown in Figure 7. The precision of the measurements is $\Delta r_1 = 0.0025$. It was obtained by calculating the standard deviation on 20 measurements points when DW is injected inside the micro-channel.

We can observe, from the obtained values for the four DTI samples that the r_1 values are always superior to those obtained for silicon smooth surface. The smooth silicon surface values represent the experimental reference case where we have complete wetting (liquid completely cover the bottom surface of DTI). For example, in the case of water and pure ethanol for the DTI 4 µm, we obtain values of 0.91 and 0.93 respectively which are significantly higher than the values obtained on smooth surface (0.86 and 0.91). These superior values indicate that wetting inside the trenches is not total and could be related to air being present in the network. Thus, the amount of reflected energy is greater than that in a purely Wenzel state, implying an increase in the reflection coefficient and non-complete wetting inside the trenches. Thus, using the different mixtures of water / ethanol, a partial and non-complete wetting was observed.

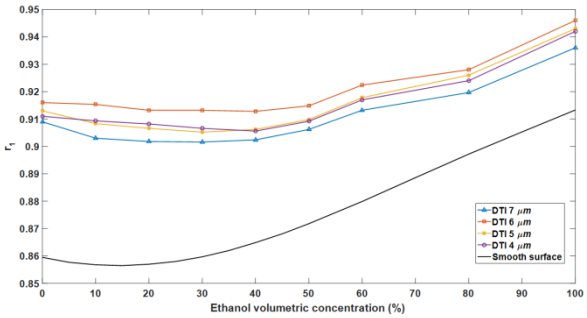

Figure 7 – Variations of the acoustic reflection coefficient r_1 on the bottom of the DTI 4, 5, 6 and 7 µm for different distilled water / ethanol mixtures injected inside the 80 µm micro-channel.

Now we will use the diluted SC1 solution. The idea behind using the SC1 is to eliminate any organic material from inside the DTI that could prevent the complete wetting. The measurement of the acoustic reflection coefficients (r_1 and r_2) are plotted with time (using MatLab program) for DTI 6 µm sample with 80 µm micro-channel (Figure 8). The measurements correspond to four phases:

- Phase 1 is the initial phase where the micro-channel is empty,
- In phase 2, the micro-channel is injected with SC1,
- Phase 3 corresponds to wetting transition after injection of air to dry the micro-channel,
- Phase 4 corresponds to the complete drying of the micro-channel and the return to the initial phase (phase 1).

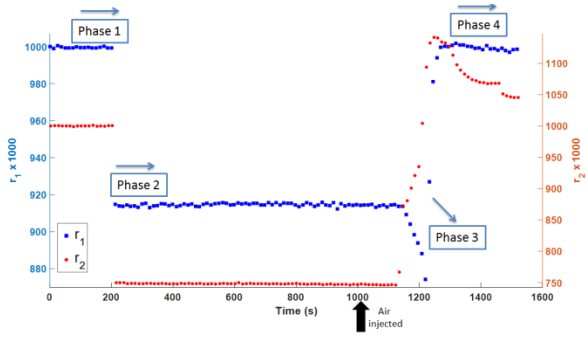

Figure 8 – Variation of the acoustic reflection coefficients r_1 and r_2 with time for DTI 6 µm with 80 µ micro-channel injected with SC1 solution: initial phase (phase 1), injection of liquid (phase 2), wetting transition (phase 3) and complete drying (phase 4)

By observing Figure 8, at phase 1 we can state that the micro-channel is empty ($r_1 = r_2 = 1$), then at t = 212 sec we can see the impact of liquid filling the micro-channel. The values of the bottom and top reflection coefficients fall instantly to reach phase 2 (r_1 = 0.92 and r_2 = 0.75). The values of the reflection coefficient r_1 obtained here are similar to the ones obtained with DW (Figure 7). This result was expected since the SC1 is highly diluted ($r_{Si/SC1}$ = 0.86). At t = 1000 sec, air is injected in the micro-channel to dry it. The liquid inside the micro-channel starts to be pushed to the outlet. At t = 1123 sec a transition from phase 2 to phase 3 takes place, r_2 increases gradually and r_1 decreases to reach a value of 0.87 at t = 1220 sec which is close to the theoretical value on a smooth surface for complete wetting ($r_{Si\ /\ SC1}$ = 0.86). Finally, a transition to phase 4 takes place where the micro-channel is completely dry and the reflection coefficients regain their original value close to 1.

A remarkable transition from phase 2 to phase 3 occurred in the case of DTI 6 µm (Figure 8) where we saw that r_1 reached a value of 0.87 which is very close to the value obtained for complete wetting ($r_{Si\ /\ DW}$ = 0.86) indicating a quasi-complete wetting behavior on the bottom surface of the DTI. The transition from phase 2 to phase 3 was accompanied by the observation (using the microscope positioned above the micro-channel) of bubbles exiting the DTI network (Figure 9.b). This confirms the scenario we proposed about trapped air pockets inside the trenches which inhibited the total wetting. The origin of these bubbles is correlated to the observation of bubbles when the SC1 was injected in the micro-channel (Figure 9.a) and inside the beaker of the prepared SC1 solution. Indeed they are due to the presence of oxygen (O_2) generated due to the decomposition of hydrogen peroxide:

$$2H_2O_2 \rightarrow 2H_2O + O_2 \qquad (3)$$

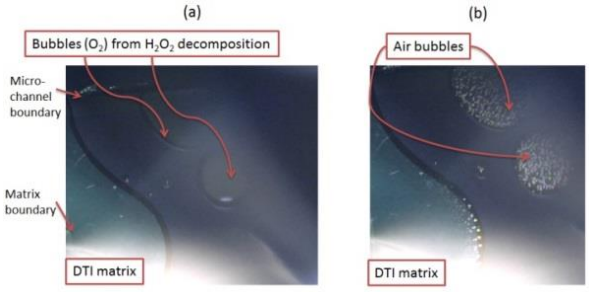

Figure 9 – (a) Observed bubbles during the injection of the SC1 solution in the micro-channel (b) air bubbles exiting the DTI network during the drying phase.

It is important to note that the transition from phase 2 to phase 3 was not always systematic. It was dependent whether the trapped air is able to exit the DTI network or not. Also, it was independent of the DTI sample as we observed it also on the DTI 4 µm with the diluted SC1 solution.

We formulated a hypothesis that the wetting transition is directly linked with the observation of O_2 bubbles in the injected solution. However, as we can see in Figure 10, a wetting transition to total wetting state for pure ethanol (r_1 = 0.91 = $r_{Si/EtOH}$) on the DTI 4 µm, with 80 µm micro-channel, could be observed during the drying phase (phase 3) without the appearance and influence of the O_2 bubbles. This wetting transition observation with ethanol indicates that this transition can be related to the pressure changes inside the micro-channel when we inject air at 1 bar (liquid is injected at 300 mbar).

To understand the pressure change effect one explanation could be formulated. The pressure is balanced between the liquid on one side (Laplace pressure), which is acting downward on the liquid air meniscus, and the

pressure generated from the trapped air pockets on the bottom of the trenches on the other side which is acting upwards on the liquid air meniscus (Figure 11). When air is injected into the micro-channel at a pressure of 1 bar, the pressure of the suspended liquid increases and pushes further on the air pockets. It reduces their volume leading to a diffusion of these pockets into the liquid and the increase in the wetted bottom surface area of the trenches (air pockets replaced by the liquid). This diffusion of the air pockets into the liquid could also explain the phenomenon observed in Figure 9.b showing tiny air bubbles exiting from the DTI network.

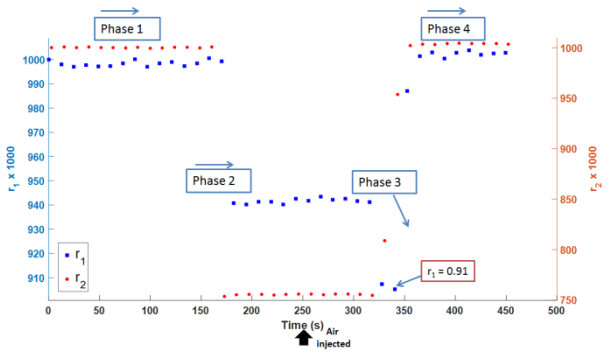

Figure 10 – Variation of the acoustic reflection coefficients r_1 and r_2 with time for DTI 4 µm with 80 µ micro-channel injected with pure ethanol: initial phase (phase 1), injection of liquid (phase 2), wetting transition to complete wetting (phase 3) and complete drying (phase 4)

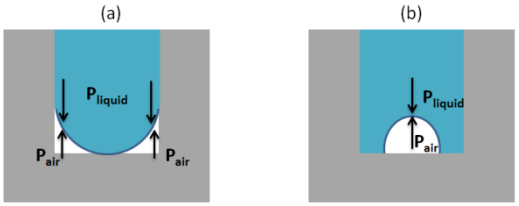

Figure 11 – Pressure equilibrium between trapped air (P_{air}) pockets and suspended liquid (P_{liquid}) inside the DTI for (a) hydrophobic surface and (b) hydrophilic surface

3.2 Pattern collapse

As we are dealing with high AR structures like the DTI, the structural deformation due to capillary forces acting on the trenches during the drying phase is highly probable. The capillary pressure is the pressure difference formed across a meniscus (Liquid-air interface). It is given as [11]:

$$\Delta P_{cap} = \frac{2\gamma \cos \alpha}{d} \quad (4)$$

With α contact angle, γ surface tension of the liquid and d width of the trench. The capillary force (F_{cap}) acting on the trench due to different filling height of the liquid (Figure 12) is then given as a product of capillary pressure multiplied by the surface area of the trench. It is mathematically written as:

$$F_{cap} = \frac{2\gamma \cos \alpha}{d} hl \quad (5)$$

We can see from Eq. (5), the impact of the AR (h/d). The higher the AR, the higher the capillary forces acting on the trenches.

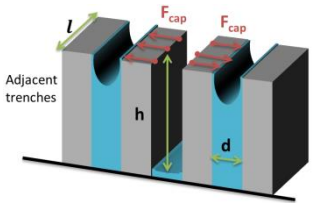

Figure 12 – Schematic of the capillary forces acting upon trenches with different liquid filling height

Since the structural deformation or pattern collapse require visualization method. We used SEM images on the four DTI samples that we used to carry out the wetting characterization measurements. The SEM images were taken at the location of the DTI matrix where we placed the micro-channel after removing the PDMS.

We can see that the pattern collapse is clearly seen on the DTI 6 µm and 7 µm (Figure 13.c and Figure 13.d respectively), and it is linked to the small rectangular pillars represented by the red arrows while the larger pillars represented by the blue arrows are intact. These pillars have dimensions of (300 x 565 nm^2) and the larger pillars have dimensions of (1.8 x 1.9 μm^2) so, we get an aspect ratio (ratio of the pillar height to its lateral dimension) of 20 and 23 for the small pillar of DTI 6 µm and 7 µm respectively while the aspect ratio for the larger pillars is 3 and 4 for DTI 6 µm and 7 µm respectively.

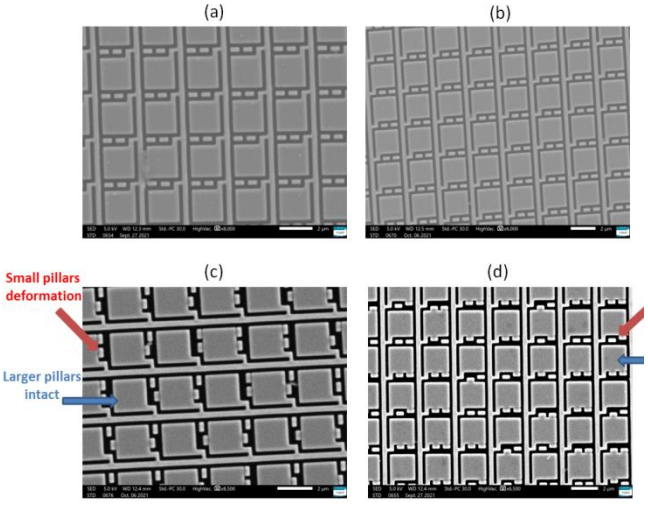

Figure 13 – SEM images of the DTI matrix showing the etched trenches (black color) and the silicon pillars (grey color) for (a) 4 µm, (b) 5 µm, (c) 6 µm and (d) 7 µm etch depth

The pattern collapse could be observed up closely by the bending of the small rectangular pillars (Figure 14.a). The smaller pillars tend to bend and attach to the larger

ones due to the formation of solid bridges [12] during liquid evaporation (Figure 14.b). These bridges could form from the oxidation of silicon into silicon dioxide (SiO_2), and act as a bond holding the structures together. The oxidation is due to the fact that we used ambient air (O_2 present) in our drying process. In industry nitrogen (N_2) drying is used to minimize this oxidation effect during the drying process. Usually to break this kind of bonds and straighten the pillars, hydrofluoric (HF) vapor cleaning is used at industry.

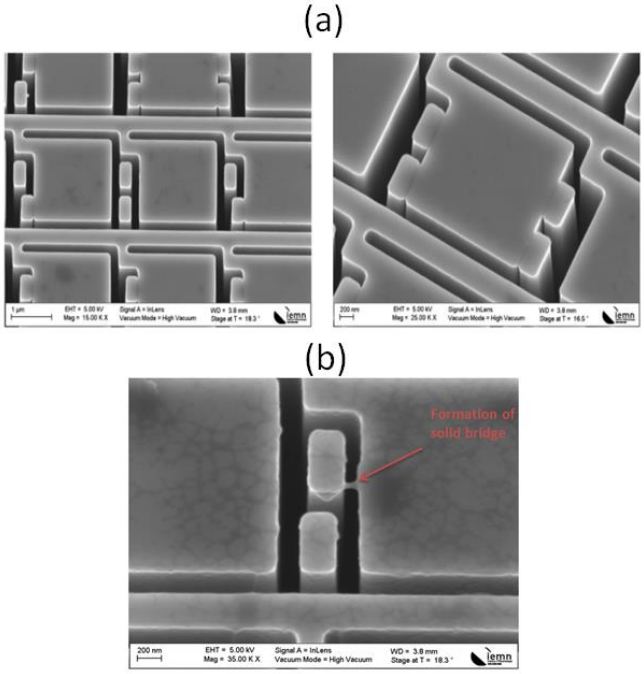

Figure 14 – (a) SEM images of the DTI 7 µm matrix showing the deformation of the small pillars (b) Formation of a solid bridge on the small pillar.

4 Conclusion

In this work, we presented the kinetic wetting characterization using acoustic reflectometry method on DTI structures using flow conditions as close as possible to those used at STMicroelectronics. With an 80 µm deep PDMS micro-channel we were able to inject different ethanol / distilled water mixtures and detect partial wetting state. Using automated acquisition technique with a MatLab program, wetting transition to quasi-complete wetting with the SC1 solution on DTI 6 µm etch depth and a complete wetting were detected on the DTI 4 µm etch depth using pure ethanol. However, this transition was not systematic and was related to pressure changes during the drying process and the exit of trapped air bubbles from the DTI network. Pattern collapse was also detected through SEM images on the high AR (20 and 23) DTI pillars.

Acknowledgements

This work was partially supported by the French Renatech network. This research work has been partially undertaken with the support of IEMN fabrication (CMNF). The authors would like to thank the Program NANO 2022 supporting the joint lab IEMN - STMicroelectronics.

References

[1] T. Young, "An essay on the cohesion of fluids," *Philos. Trans. R. Soc. London*, vol. 61, 1805, pp. 65–87.

[2] A. B. D. Cassie, "Contact angles," in *Discuss. Faraday Soc.*, vol. 3, 1948, pp. 11–16. [Online]. Available: DOI https://doi.org/10.1039/DF9480300011

[3] R. N. Wenzel, "Resistance of solid surfaces to wetting by water," *Ind. Eng. Chem.*, vol. 28, no. 8, 1936, pp. 988–994.

[4] Park, Sohyun and Kim, Jooyoun and Park, Chung, "Superhydrophobic Textiles: Review of Theoretical Definitions, Fabrication and Functional Evaluation," *Journal of Engineered Fibers and Fabrics*, vol. 10, 2015.

[5] Chen, Y. , Ren, W. , Mu, X. , Zhang, F. , Xu, Y., "Flow inside Micro-Channel Bounded by Superhydrophobic Surface with Eccentric Micro-Grooves," *World Academy of Science, Engineering and Technology, Open Science Index 129, International Journal of Mechanical and Mechatronics Engineering*, vol. 11,9, 2017, pp. 1579–1584.

[6] Vrancken, N., Li, J., Sergeant, S., Vereecke, G., Doumen, G., Holsteyns, F., Chen, C., Terryn, H., De Gendt, S., & Xu, X., "In-situ ATR-FTIR for dynamic analysis of superhydrophobic breakdown on nanostructured silicon surfaces," *Scientific reports*, vol. 8,1, 2018, p. 11637.

[7] Chen, Yuanmiaoliang and Wang, Zhangxin and Jennings, Kane and Lin, Shihong, "Probing Pore Wetting in Membrane Distillation Using Impedance: Early Detection and Mechanism of Surfactant-Induced Wetting," *Environ. Sci. Technol. Lett.*, vol. 4,11, 2017, pp. 505–510.

[8] D. Zamani, K. Dhane, O. Mahdavi, M. Anthony, J. Yan, and F. Shadman, "surface cleaning of small structures during spin rinsing of patterned substrates," *Microelectronic engineering*, vol. 108, 2013, pp. 57–65.

[9] Virgilio, C. , Carlier, J. , Campistron, P. , Toubal, M. , Garnier, P. , Broussous, L. , Thomy, V. , Nongaillard, B., "Wetting Characterization of High Aspect Ratio Nanostructures by Gigahertz Acoustic Reflectometry," *International Journal of Mechanical and Mechatronics Engineering*, vol. 10,3, 2016, pp. 506–511.

[10] Christophe Virgilio, "Caractérisation du mouillage de surfaces micro/nanostructurées par méthode acoustique haute fréquence : application aux traitements humides dans l'industrie de la microélectronique. Micro et nanotechnologies/Microélectronique," Université de Valenciennes et du Hainaut-Cambresis, 2017.

[11] Peter, Daniel, "Pattern Collapse - the Mechanical Stability and Solid Bridging of Semiconductor Nanostructures," 2010.

[12] R. L. Alley, G. J. Cuan, R. T. Howe and K. Komvopoulos, "The effect of release-etch processing on surface microstructure stiction," *Technical Digest IEEE Solid-State Sensor and Actuator Workshop*, 1992, pp. 202–207.